THE DEVELOPMENT OF SPECIAL INSTRUMENTATION AND PROCEDURES FOR NUCLEAR SCIENCE APPLICATIONS USING THE UNIVERSITY OF MANITOBA SPIRAL RIDGE CYCLOTRON FACILITY

by

Ravi Prakash

A Thesis
Presented to the University of Manitoba
in Partial Fulfillment of the
Requirements for the Degree of
Master of Science
in
Nuclear Physics
The University of Manitoba

Winnipeg, Manitoba, 1985

THE DEVELOPMENT OF SPECIAL INSTRUMENTATION AND PROCEDURES FOR NUCLEAR SCIENCE APPLICATIONS USING THE UNIVERSITY OF MANITOBA SPIRAL RIDGE CYCLOTRON FACILITY

BY

RAVI PRAKASH

A thesis submitted to the Faculty of Graduate Studies of the University of Manitoba in partial fulfillment of the requirements of the degree of

MASTER OF SCIENCE

ACKNOWLEDGEMENTS

I would first and foremost like to thank my supervisor, Dr. Jasper McKee for his patience and support of my work over the last two years. My thanks also go out to Jim Birchall, Matthew Al-Ghazi, Claude Lapointe and Nelson Videla for their assistance during my time here. John Lancaster, Jim Lanfear and all the members of the workshop, computer and support staff were invaluable in developing the work described herein. These projects would also have been far more difficult to develop if not for the assistance and advice of Dr. Frank Hawthorne, Dr. W. Woodbury and Dr. S. Oh of the University of Manitoba, Dr. Tom Cahill of the University of California at Davis and Dr. R.D. Vis of Vrije Universiteit, Amsterdam.

ABSTRACT

The Proton Induced X-Ray Emission (PIXE) technique has become a practical means for trace element analysis since 1968 and has come to be accepted as a viable method for the detection of several elements simultaneously to as good an accuracy as a few parts per billion (ppb). It was first reported in 1970 that a focussed beam of protons with a spot size on the order of 3μm was produced at Harwell to employ the PIXE technique on a fine scale.

For several years now the University of Manitoba spiral ridge cyclotron has been used for K X-ray PIXE analysis, and the design for a micro-PIXE facility is presented here.This facility is presently under construction and will be on-line late in 1985. It is capable of producing a beam spot of 10 μm diameter for the full range of proton energies produced by the cyclotron, 20-50 MeV.

The technique of proton scattering radiography has been known for some time, but its applications have been few and far between. Recently this process has been applied to the study of barley grains in conjunction with the Department of Plant Sciences at the University of Manitoba, and the first results are presented herein.

The upgraded University of Manitoba Cyclotron Laboratory is capable of producing deuteron beams of up to 26 MeV. However, this beam has quite a large energy spread, up to one MeV. Thus a single turn extraction system for deuterons has been designed to produce deuterons of up to 15 MeV with approximately a 50 keV energy spread.

TABLE OF CONTENTS

Acknowledgements i

Abstract ii

Table of Contents iv

List of Figures vi

I Development of a Proton Analytical Technique for Trace Investigation 1

I.1 Proton Induced X-ray Emission (PIXE) 1

I.2 Micro-PIXE 6

I.3 Potential Applications of the Manitoba Microprobe 7

I.4 Design of the Manitoba Microprobe 11

I.5 Collimation 13

I.5.1 Optics 17

I.5.2 Detection System 20

I.5.3 Results 22

I.5.4 Final Colimator Design 25

I.6 Focussing 27

I.7 Summary 29

II Proton Scattering Radiography 30

II.1 Introduction 30

II.2 The Barley Grain 36

II.3 Experimental Procedure and Results 37

II.4 Summary 40

III Design of a Separated Turn Extraction System
For Deuterons 41
III.1 Introduction 41
III.2 Stage 1 - Collimators 42
III.3 Stage 2 - Skimmer Probes 46
III.4 Skimmer Probe Design 48

Summary and Conclusion 51

Bibliography 54

LIST OF FIGURES

1. Atomic Model, Showing Electron Transitions That May Follow Electron Vacancies 3

2. Side View of Micro-PIXE Beam Line and Corresponding Beam Profile 12

3. Profiles of the Four Collimator Configurations Tested 14

4. Floor Plan of the University of Manitoba Cyclotron Laboratory 15

5. Experimental Arrangement For Slit Scattering Run .. 16

6. Schematic and Optics of Slit Scattering Run 19

7. Electronics For Slit Scattering Run 21

8. 35 MeV Beam Profiles 23

9. 22.9 MeV Beam Profiles 24

10. Section of 70 μm Collimator 26

11. Section of a Quadrupole Lens and Stand 28

12. The Intensity Pattern Behind an Edge As a Result of Proton Scattering 35

13. Experimental Arrangement for Proton Radiography on ´D´ Line 38

14. Proton Radiograph of Barley Tip 39

15. Faraday´s Disk 44

16. Schematic of Separated Turn Extraction System For Deuterons 45

17. 15^{o} Pole Tip 49

CHAPTER I

DEVELOPMENT OF A PROTON ANALYTICAL TECHNIQUE FOR TRACE ELEMENT INVESTIGATION

I.1 PROTON INDUCED X-RAY EMISSION (PIXE)

If one considers the Bohr model of the atom, one postulates the electrons to be bound in discrete shells about the nucleus by electromagnetic interactions, the population of these shells being determined by the Pauli Exclusion Principle (Ti78). The various shells and subshells defined by this theory are illustrated in figure 1. Removing an electron from one of the inner shells places the atom in an excited state. In order to minimize the energy, an electron from one of the outer shells will drop down to fill the vacancy, fluorescing, or releasing an X-ray photon of a well defined-wavelength in the process. These transitions are labelled by the shell letter of the final state of the decaying electron. As the shell structure is unique for each atom, the energy of the emitted X-ray identifies not only the transition, but also the element in question. These X-rays appear as distinct peaks on the X-ray

continuum, their position, and thus their wavelength, allowing one to identify the element in which the transition occurred (Wo73).

Inner shell ionization, as described above, requires a means of exciting the target atom. This process may involve primary excitation by charged particles or secondary excitation by some form of electromagnetic radiation (Wo73). The PIXE process falls under the former category.

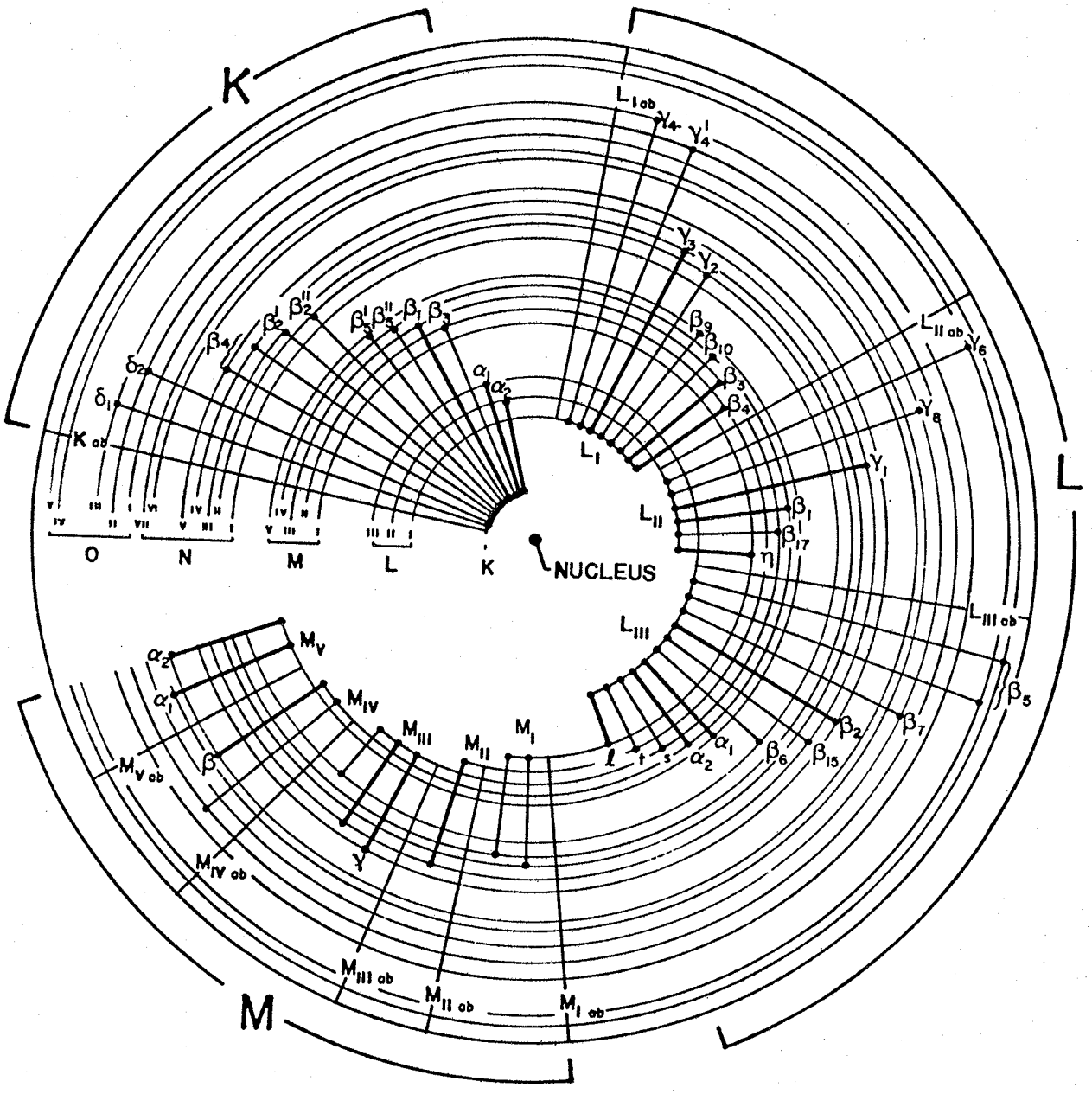

Figure 1: Atomic Model, showing electrontransitions that may follow electron vacancies.

Electrons and protons are most commonly used in primary excitation systems, although heavier ions are also used (Wo73). Upon striking the target, the bombarding particles undergo several decelerating collisions which produce X-rays in a continuous spectrum called the bremsstrahlung, or background. By the following relationship (La81),

$$I \propto \frac{z^2 Z^2}{M^2} \qquad \text{(I-1)}$$

where Z is the atomic number of the target material and z and M are the charge and mass, respectively, of the bombarding particle, the intensity, I, of the background radiation is inversely proportional to the square of the mass of the incoming particles. The intensity of the bremsstrahlung produced by protons is thus far less than that produced by electrons since the proton mass is approximately two thousand times greater than that of the electron.

Whereas an electron beam can interact with inner shell electrons only through inelastic collisions, proton beams can also remove electrons by means of another process. If the velocity of the proton is approximately that of the inner shell

electron, they may temporarily form a neutral hydrogen atom which essentially acts independently of the electron's parent atom. Although this state is unstable, it generally does not decay until the proton has carried the electron free of the atom (La81).

PIXE is a non-destructive technique, providing reproducibility of any given test results with any given sample. The process is easily automated, allowing for the rapid analysis of a large number of samples. Advantages shared with other forms of X-ray energy spectrometry include the ease of identification of X-ray spectra and the fact that many elements of the periodic table can be analyzed simultaneously with great precision. These factors, in addition to the above-mentioned advantage over electron induced X-ray emission techniques indicate why the PIXE process has come to be accepted as a powerful means of trace element analysis with applications in many fields (Pr85).

I.2 MICRO-PIXE

The PIXE technique is up to three orders of magnitude more sensitive than electron induced X-ray emission, partly due to the reduced background (La81). The advent of microbeams used in conjunction with this form of analysis can improve the detection limit even further (Ca80). It was first reported in 1970 that a focussed beam of protons with a spot size of the order of 3 μm was produced at Harwell (Co72) in order to use the PIXE technique on a fine scale. Collimated microbeams with spot sizes of several μm have existed since 1953 (Zi53) and have been combined with PIXE techniques effectively (Co79). However, despite several notable advances, particularly in the slit design of Nobiling et al (No75), collimated microbeams, when compared with focussed microbeams, still exhibit several inherent disadvantages, not the least of which are the greatly reduced beam currents and larger spot sizes. Both collimated and focussed microbeams are used and new micro-PIXE facilities appear each year. Beam spot size varies from facility to facility and relates to the analysis being performed (Pr85).

I.3 POTENTIAL APPLICATIONS OF THE MANITOBA MICROPROBE

For several years now the University of Manitoba spiral ridge cyclotron has been used for K X-ray PIXE analysis (Wi77). The high energy of the protons from this machine (20 to 50 MeV) does not restrict the PIXE analysis to the study of the L X-rays of medium and heavy-Z elements. Due to the typical energies of microbeam systems currently on line (of the order of a few MeV), it has only been possible to produce the L X-rays of these elements. Unfortunately, there is generally considerable overlap in the X-ray spectra between these X-rays and the K X-rays of lighter elements. This problem, as well as the higher background of these low energy machines will be bypassed by the Manitoba microprobe, as one will be able to study the relatively 'clean' K X-ray spectra of these heavier elements (Pr85). There is already a great demand for these capabilities, both in further research already in progress involving bulk PIXE analysis and in emerging fields.

Down's Syndrome can result from trisomy 21, or a damaged chromosome. Recently, the Department of Human Ecology at the University of Manitoba has been working with us to study the relevance of trace elements in the hair of Down's Syndrome children. Hair samples from infants with the syndrome and from

normally-developing children have been subjected to bulk PIXE analysis. Indications were found that behavioral symptoms of Down's Syndrome are related to certain trace element levels, most especially with respect to zinc (Ba82). Whereas further bulk PIXE analysis is also called for, micro-PIXE will allow the trace element distributions to be followed along the length of either a child's or a mother's hair in order to observe correlations between changing nutrition levels in the mother and the elemental composition of hair from the Down's Syndrome infants.

70% of the world's cesium supply is located in Manitoba. It is anticipated that there will be a great interest in mining this element in the near future. However, little was known prior to 1978 of the distribution of cesium within the body (Mc81). Studies have been carried out in conjunction with the Department of Therapeutics and Pharmacology at this university of mice injected with various doses of CsCl. Samples from certain organs such as the heart, liver and brain are then prepared and analysed for cesium content. Absolute determinations are made by doping samples with known amounts of dysprosium (Mc81). It is, however, sometimes desirable to study the variation in uptake of cesium across and through an organ such as the heart. This procedure, which will be possible with the microprobe, relates to both diagnosis and

therapy.

A new study, also involving cesium, concerns the preferential absorption of that element by tumors as opposed to healthy cells. There has been sufficient indication of this to use Cs as a tracer in tumors in mice. Application of the microprobe at a cellular level here would be useful in examining detailed uptake of cesium. A greater understanding of the blood flow in the tumor could be gained. Tumors rapidly outgrow their blood supply and as a result the centre is often left without oxygen, but survives nonetheless. As the cesium can only reach the tumor from the bloodstream, an analysis of the cesium content in a tumor could give some indication of the efficiency of the blood transportation system (Mc83).

As the conditions of crystallization change for some given mineral, the composition of that mineral changes with crystal growth. Thus, bound into the structure of a mineral is the history of its formation (Ha84).

It has been possible for some time to observe the changes in bulk elements using electron probes. Until now, however, there has been no means of determining the behaviour of trace elements in these crystals. One had to accept either the relatively poor resolution of the Si(Li) detector or the low efficiency of the crystal spectrometer in observing the L

X-rays of these elements which largely consist of the rare earths (Ca80, Le82, Le84, Pr85). The Manitoba microprobe will allow the observation of the K X-rays of these elements, thus providing improved identification of the peaks, much better resolution and hopefully lower background.

I.4 DESIGN OF THE MANITOBA MICROPROBE

The University of Manitoba Microprobe Facility has been designed in two stages: collimation and focussing. The final beam line and corresponding beam profile are depicted in figure 2.

Collimation begins with a simple 1mm water-cooled brass collimator mounted on the beam line to cut off much of the excess beam. Downline from this are two orthogonal sets of collimators, each consisting of a pair of water-cooled slits with a 70μm gap.

The second phase of the microprobe will focus the beam on target using four quadrupole magnets arranged in the configuration called the "Russian Quadruplet" of Dymnikov et al (Dy65), wherein the inner pair and the outer pair of magnets each have the same pole tip magnetic field strength.

This arrangement is capable of producing a beam spot of 10 μm for the full range of proton energies produced by the cyclotron, 20 to 50 MeV.

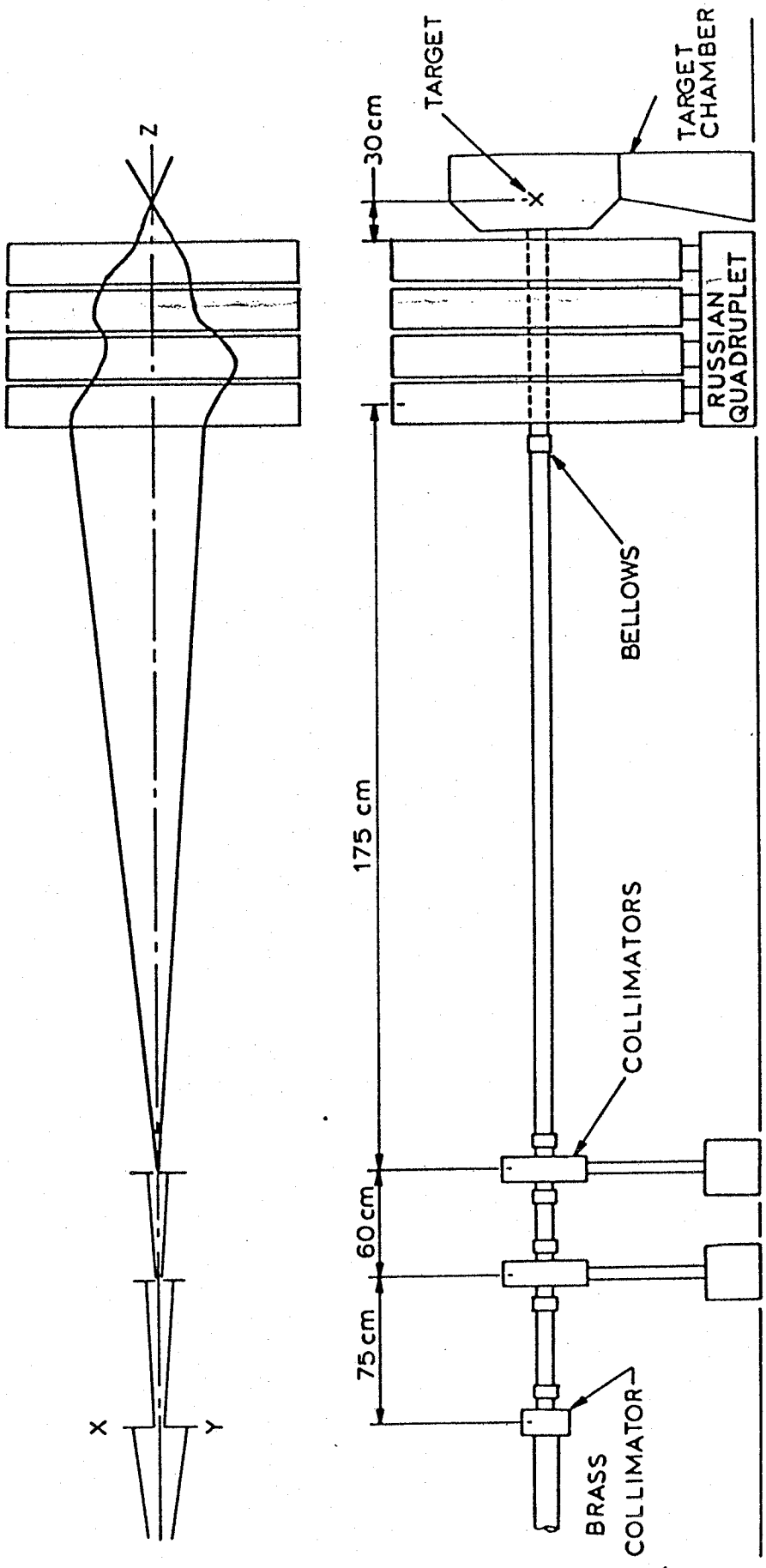

Figure 2: Side View of Micro-PIXE Beam Line and Corresponding Beam Profile

I.5 COLLIMATION

The four configurations considered for the two 70μm collimators are illustrated in figure 3. These four collimators were made and tested to determine which configuration minimized scattering of protons from the edges of the slits. The slits were tested at a 1 mm gap width, this separation being measured by means of a travelling microscope. The analysis was done on ´C´-line in the cyclotron laboratory, as shown in figure 4, the experimental arrangement is shown in figure 5.

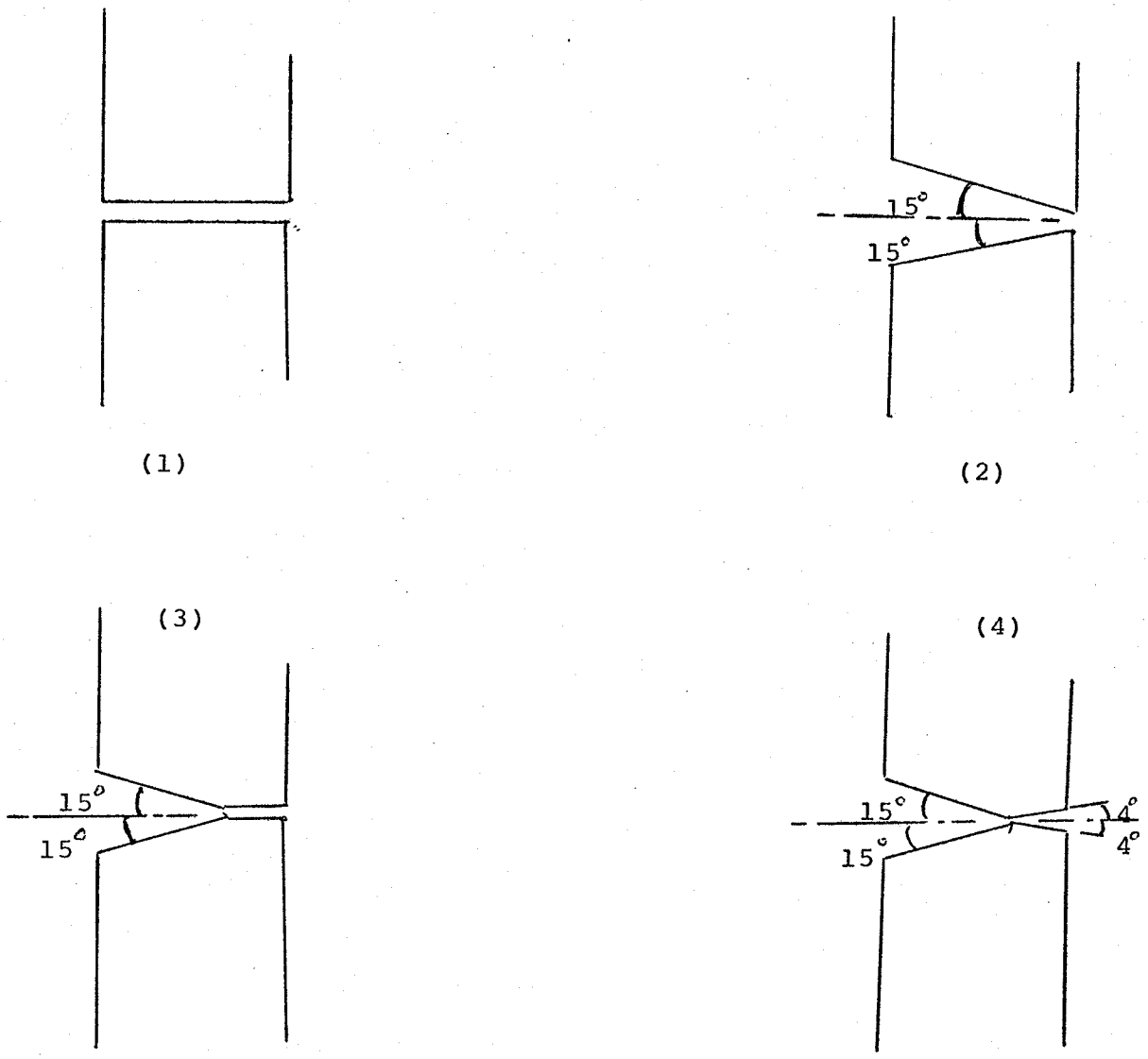

Figure 3: Profiles of the four collimator configurations tested. The incoming proton beam is from the left in each case.

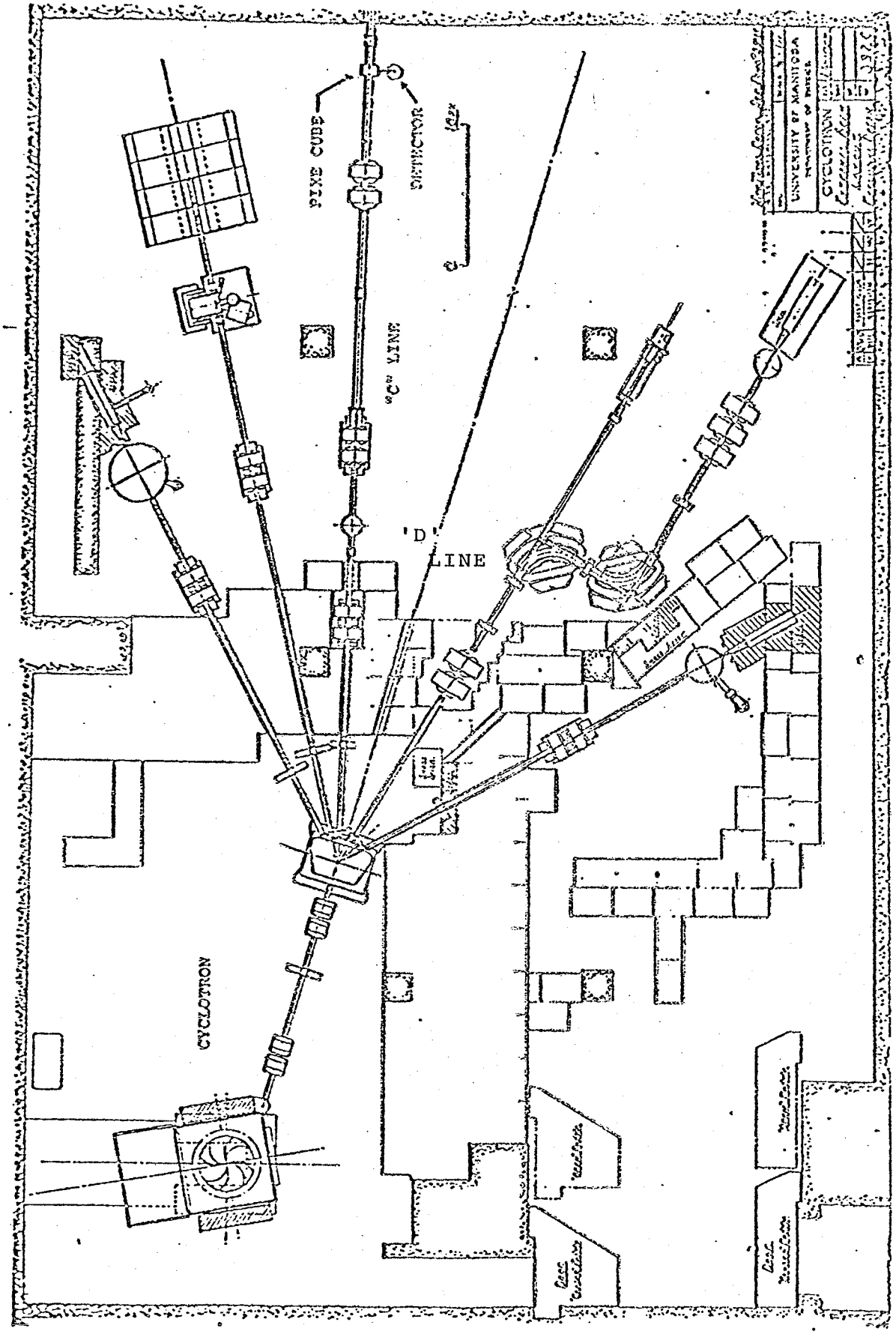

Figure 4: Floor Plan of the University of Manitoba Cyclotron Laboratory

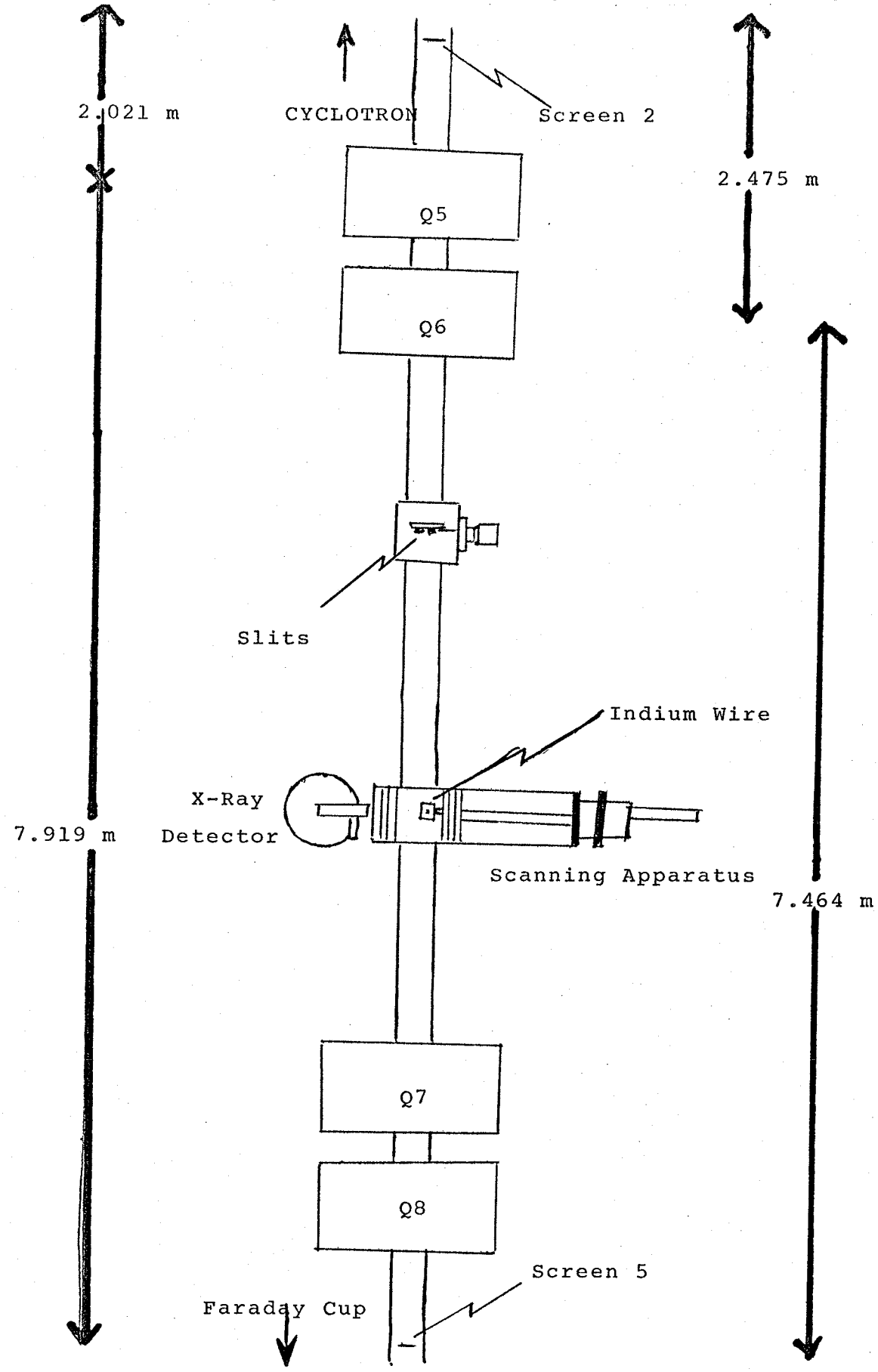

Figure 5: Experimental arrangement for Slit Scattering Run

I.5.1 Optics

Parallel beam optics were required for the slit scattering experiment in order to minimize the divergence of the beam. In order to achieve this, the beam was first focussed on screen 2 (see figure 5), and then the beam was focussed on screen 5 using only the magnetic quadrupole singlets Q5 and Q6. For either of these quadrupoles, the relationship illustrated in figure 6 applies to their respective focal plane. For small values of α and φ,

$$\alpha \cong h/(L_1) \qquad \text{(I-2)}$$

$$\varphi - \alpha \cong h/(L_2) \qquad \text{(I-3)}$$

giving

$$\varphi \cong h/(1/L_1 + 1/L_2) \qquad \text{(I-4)}$$

therefore,

$$\alpha/\varphi = H_\alpha/H_\varphi = H_p/H_f = I_p/I_f \qquad \text{(I-5)}$$

$$I_p/I_f = (1 + L_1/L_2)^{-1} \qquad \text{(I-6)}$$

where H refers to the pole tip magnetic field strength and I is the current in the magnet coils that produces this field for a parallel (p) or focussed (f) beam, as indicated by the subscript.

It was calculated that the factors (I_p/I_f) by which the currents in the coils required to produce a focussed beam on screen 5 had to be reduced in order to produce a parallel beam are 0.7967 for Q5 and 0.7510 for Q6.

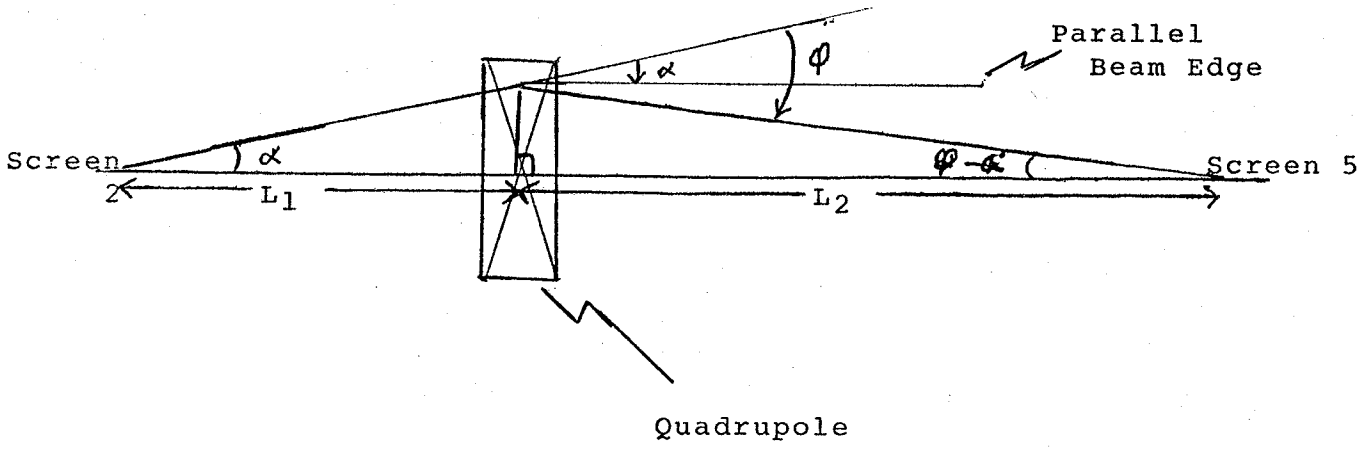

Figure 6: Schematic and optics of Slit Scattering Run

I.5.2 Detection System

The detection system consisted of a 1 mm thick indium wire mounted vertically (parallel to the slits). Indium was used because of its large PIXE cross-section. This wire was then scanned across the beam at regular intervals, the PIXE emission being recorded by an intrinsic germanium X-ray detector. A window was established which was centred on the K line of indium, and the ratio of the counts in this window to the cumulative stripping foil charge was recorded as a function of position. The electronics for the experiment are shown schematically in figure 7.

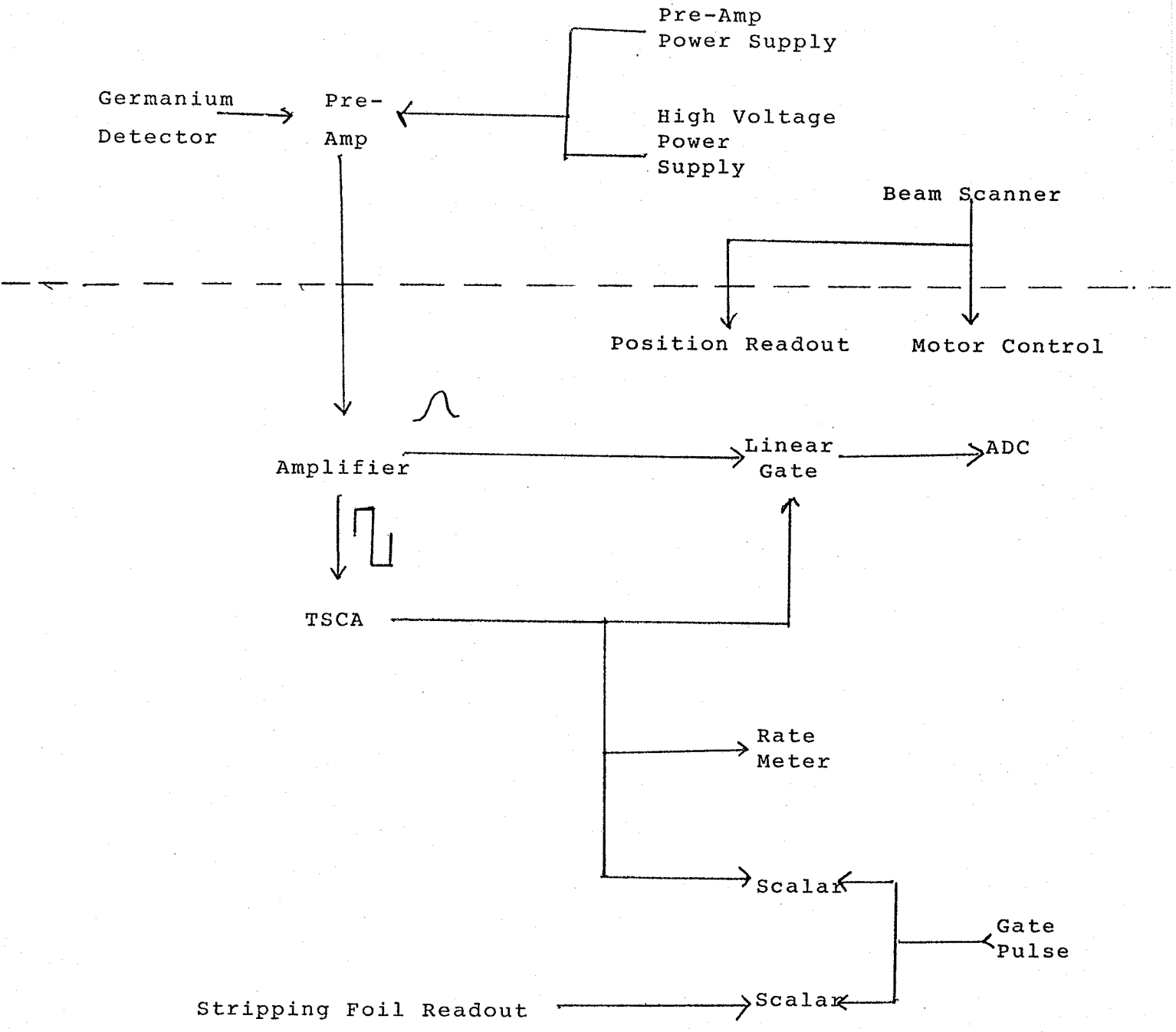

Figure 7: Electronics for the Slit Scattering Run

I.5.3 Results

Two runs were carried out with each slit, one at 35 MeV and one at 22.9 MeV. The results of these two runs are shown in figures 8 and 9. They show that collimator 4 has the least slit edge scattering, followed by collimators 3, 1 and 2 in that order. It was also observed that the performance of all the slits was improved at the higher energy.

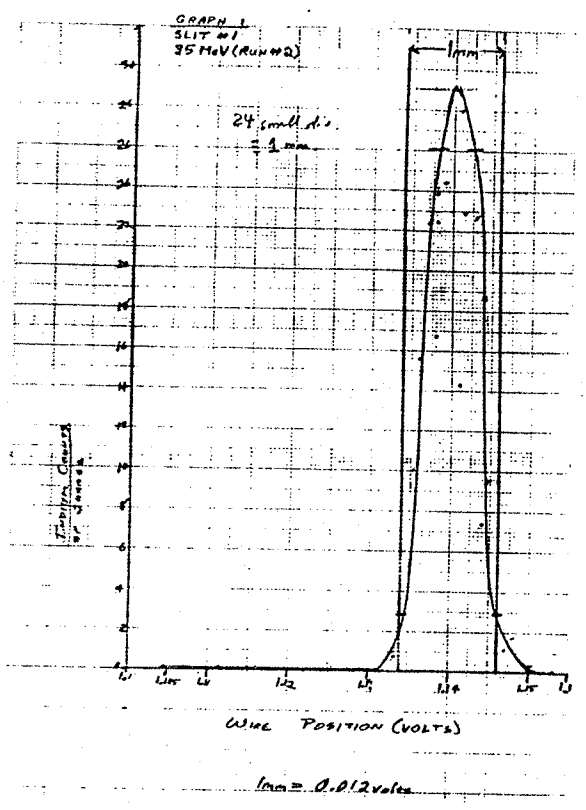

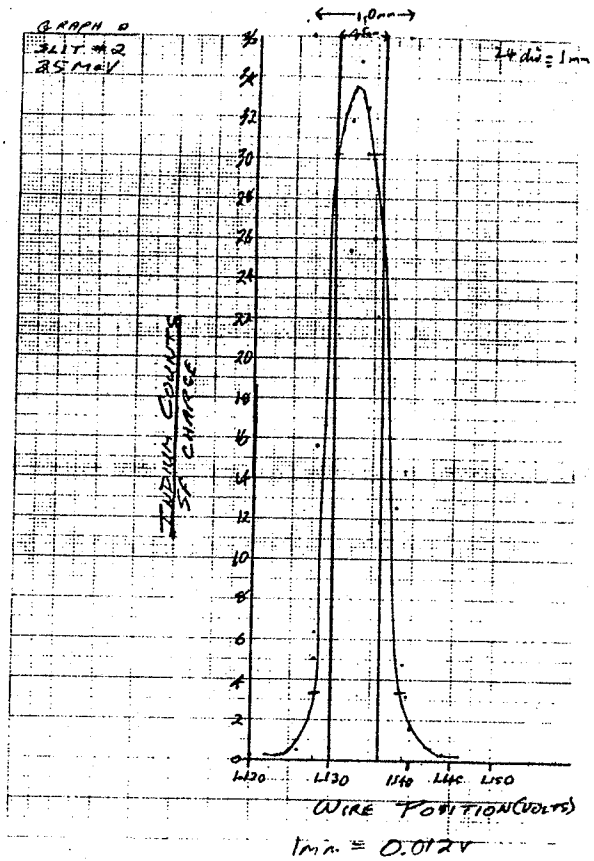

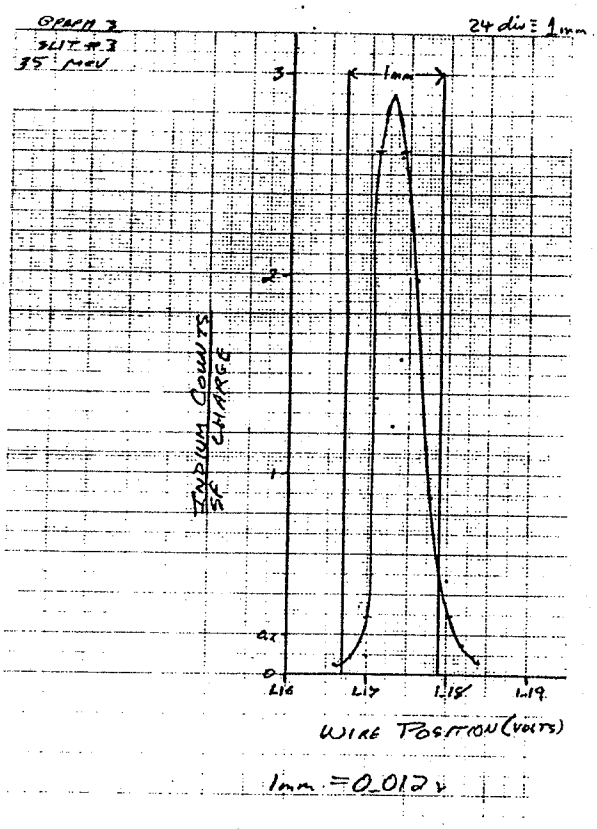

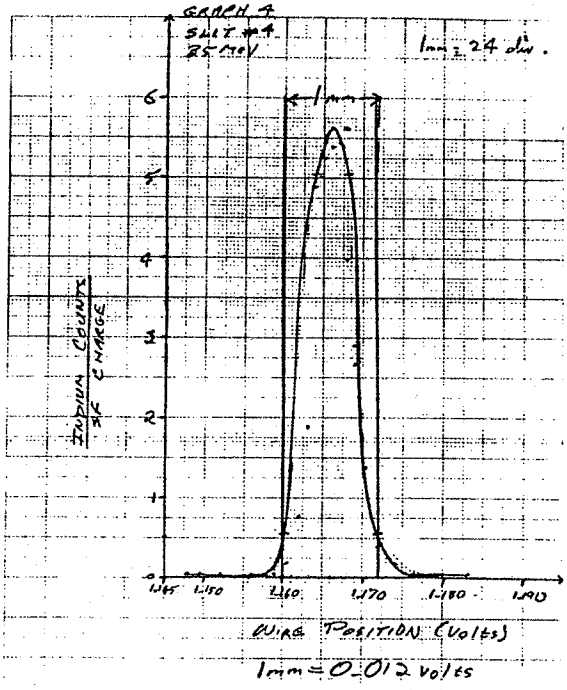

Figure 8: 35 MeV Beam Profiles

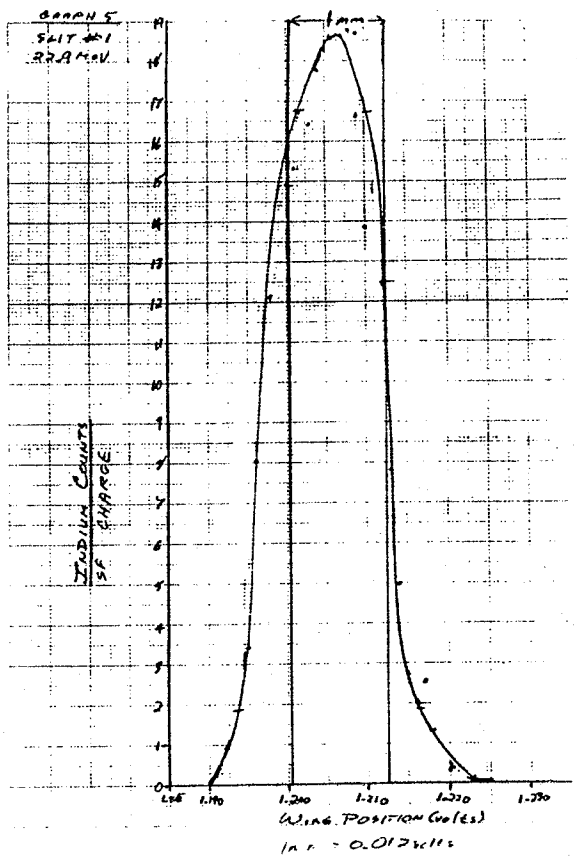

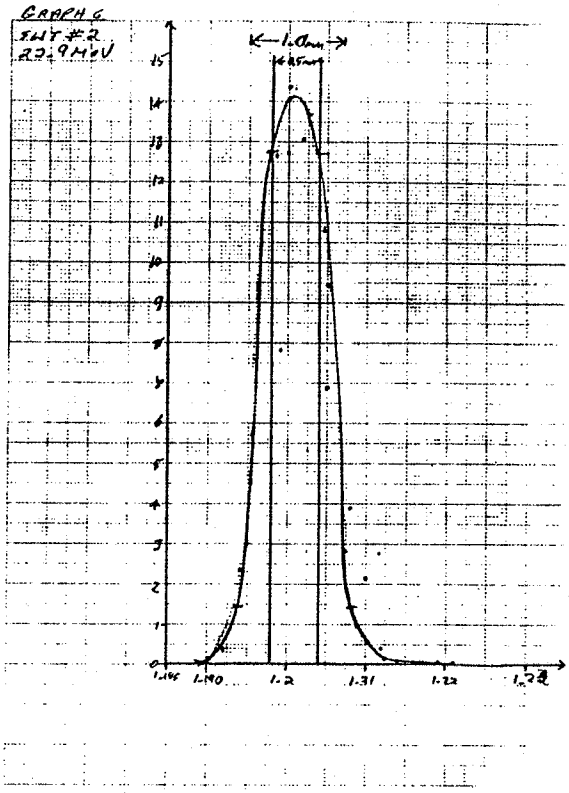

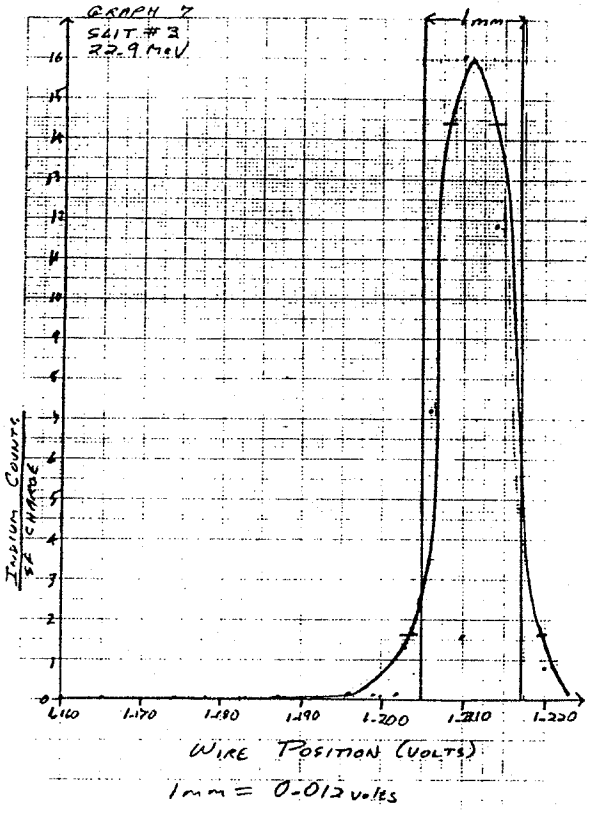

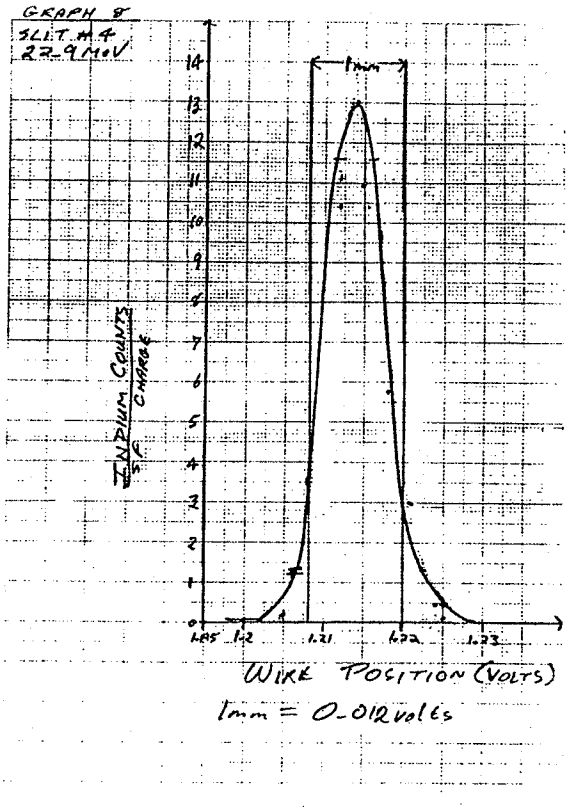

Figure 9: 22.9 MeV Beam Profiles

I.5.4 Final Collimator Design

A water-cooled collimator unit has been designed, constructed and tested using the slit design due to Nobiling (No75). The collimator was nickel. A schematic of the first stage of the microprobe is shown in figure 10. Two such units are now ready to be used in the microprobe facility.

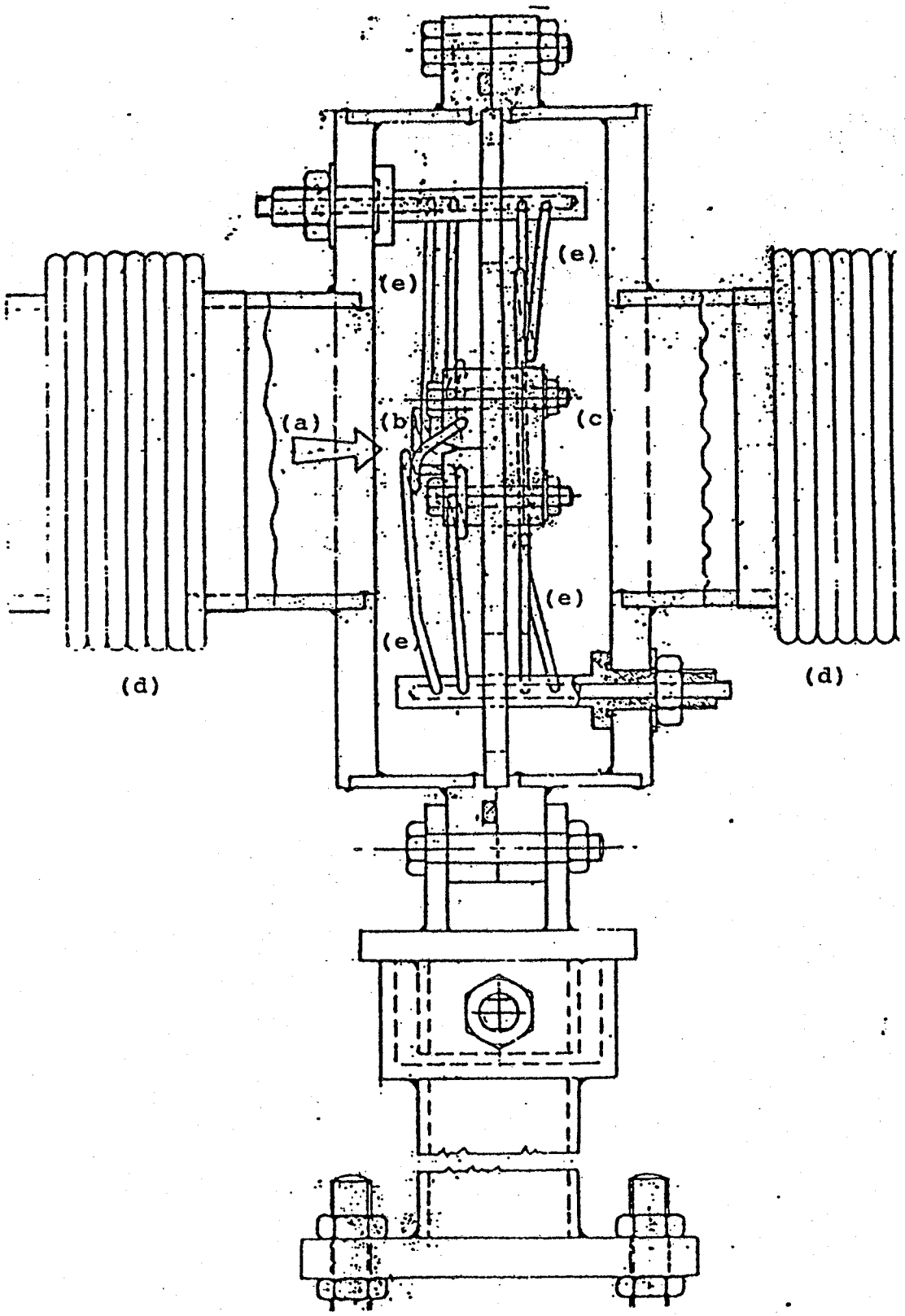

Figure10: Section of 70μm Collimator

a)Beam Direction b)Horizontal Slits c)Vertical Slits
d)Bellows e)Water Cooling Lines

I.6 FOCUSSING

A cross-section of the design of the magnets used in the second stage of the microprobe is shown in figure 11. Each magnet has a 5.08 cm gap width from pole tip to pole tip, to an accuracy of 25 μm. 220 turns of 1/4" water cooled copper wire encircle each pole piece. The pole pieces themselves are made of Armco steel, which the CRC Handbook of Chemistry and Physics (56th edition) states has similar properties to 45 permalloy, including very low hysteresis loss. Armco steel also has very low residual magnetic fields (Oh84).

The pole tips are circular approximations to the hyperbolic pole tips required to produce an ideal quadrupole field. The curvature of the pole tips was selected so as to minimize the spherical aberration.

The stand allows for correct positioning of each magnet along the optical axis. All four magnets will be mounted on a 4′ by 8′ isolation table to minimize movement due to external vibrations.

Currently, one of the quadrupole magnets has been completed and is being wound. The remaining three magnets are nearing completion.

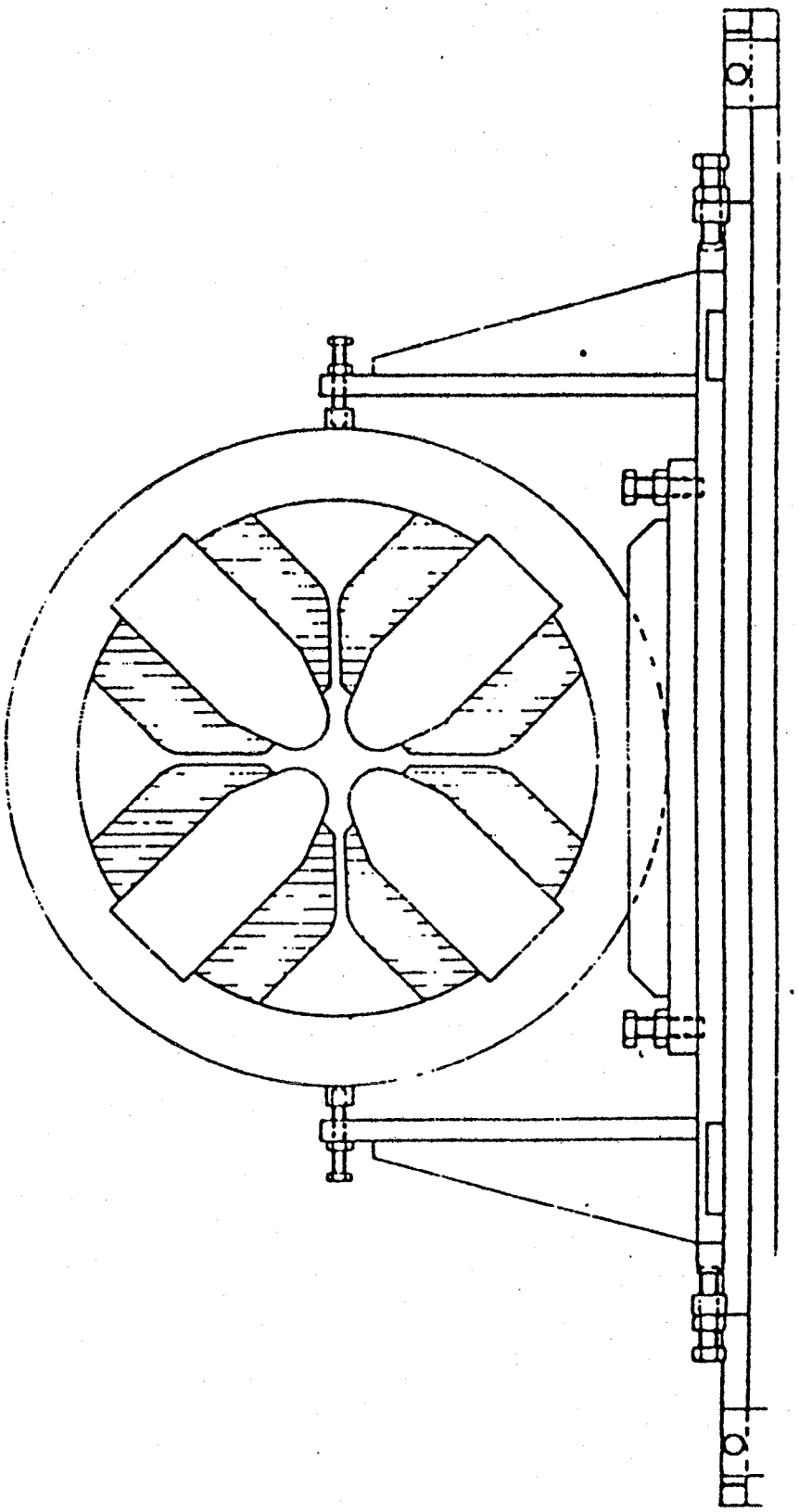

Figure 11: Section of a Quadrupole Lens and Stand

I.7 SUMMARY

Recently proton microprobes have shown promise in light element analysis at very low concentrations. With the advent of high energy microbeams many new avenues have opened up for the study of trace concentrations of medium and high-Z elements. A target chamber currently being designed for use with the Manitoba microprobe will retain considerable flexibility for future modifications, such as complementing the currently available intrinsic germanium detector with a Si(Li) detector and a crystal spectrometer. It is clear from looking at the past several years that flexibility in any microprobe facility is essential because of the diversity of its possible applications (Pr85).

CHAPTER II

PROTON SCATTERING RADIOGRAPHY

II.1 INTRODUCTION

In the nineteen-fifties, photographic films were used in accelerator laboratories to locate the position of a particle beam. A decade later Koehler suggested three methods for the use of films in producing proton radiographs (We75).

The most basic process relies upon the fact that if an object of a thickness greater than the range of the incident protons is placed in front of a photographic film, a shadow in the shape of the object will appear on the developed film.

The second method produces shaded radiographs of objects whose thickness is less than the range of the bombarding particles, much akin to X-radiographs. This is due to the fact that some fraction of the particles will undergo an exponential absorption with increasing thickness.

Considerable research has been conducted into a process known as marginal range radiography. It was observed that the proton flux decreases rapidly with small changes in the thickness of a target whose thickness is near the range of the bombarding particles in that particular substance. Thus if a film was placed next to such an object being irradiated one could detect changes of the order of 0.05% of the total thickness of the object (We72,Ko68).

From his studies, Koehler observed that proton radiography is insensitive to variations in the chemical composition within the target and that it in fact records changes in density in a sample (Ko68). Recent developments in this field have been made by Steward who studied soft tissue samples by means of marginal range proton radiography. Steward noted that heavy ions are better suited to the imaging of soft tissues than are X-rays (St79).

In 1972 West and Sherwood made a major development in the field of proton scattering radiography.

A thin object is placed so as to block a part of an incoming parallel proton beam and a film is positioned so as to intercept both the direct beam and the 'shadow' beam scattered by the object. Processing of the film after irradiation shows that all areas away from the edge of the object, either in

shadow or directly illuminated, are uniformly exposed with an intensity I_0. Protons that pass through the object are scatttered, the net effect being that the average intensity within the shadow region is the same as in the directly illuminated region, this intensity being I_o. At the edge itself, half of the normal area from which the scattering would occur is not blocked by the object and so one gets approximately half of the normal intensity (0.5 I_o). Just outside the edge one has not only the direct (unscattered) proton flux, but also an increase in flux due to protons scattered from just inside the edge. Thus the intensity increases to approximately 1.5 I_o. These two variations are seen as light and dark lines which are easily detected since the difference in intensity, ΔI, between these two bands is on the order of I_o. This process is shown in figure 12 (We72).

Thus, the outstanding feature of proton scattering radiography is that, while an X-radiograph has different shadings corresponding to different thicknesses, proton scattering radiography shows outlines of objects at sudden discontinuities in thickness, even if such a discontinuity is blocked by another part of the object.

The relaxation length of the intensity discontinuity, ΔI, depends upon the distance of the film from the edge and upon the average (root mean square) projected scattering angle θ_s, given by

$$\theta_s = (15/pc\beta) \quad (t/x)^{\frac{1}{2}} \qquad \text{(II-1)}$$

for singly charged particles (We72), where p is the momentum of the particle in MeV/c, t is the thickness of the material comprising the edge and x is the radiation length of the material for protons corresponding to the momentum p.

If the film is a distance l behind the edge, one observes that the intensity discontinuity is clearly visible for $l\,\theta_s >$ 0.05 mm and that it can be observed through enlargement for values of $l\,\theta_s$ as much as five times smaller than this minimum. However, the discontinuity inexplicably disappears for $l\,\theta_s$ smaller than this (We72).

Edge enhancement such as described above is attainable with X-rays if the radiograph is recorded on a charged selenium plate. Dusting the plate with a fine powder shows the modified charge distribution. This process is known as xero-radiography

and is used widely for xeromammography (We75). However, this edge pattern is characteristic of the recording device and not of the process itself.

Proton scattering radiography does not suffer from some of the drawbacks of X-radiography, such as extreme sensitivity to such factors as the energy, material and exposure. An easily attainable change in thickness detection limit of 1 to 2% compares favorably with X-radiography (We75). Proton scattering radiography, and to a lesser extent xero-radiography, illustrate spherical and cylindrical edges with other detail that X-radiographs cannot. They can also show muscle and tissue detail largely unseen in X-radiographs (We75).

Restrictions on the process include the above-mentioned limit to $l\theta_s$. Also, for very large l and for low proton energies, the dark and light bands tend to broaden, resulting in the loss of much of the surrounding detail (We75).

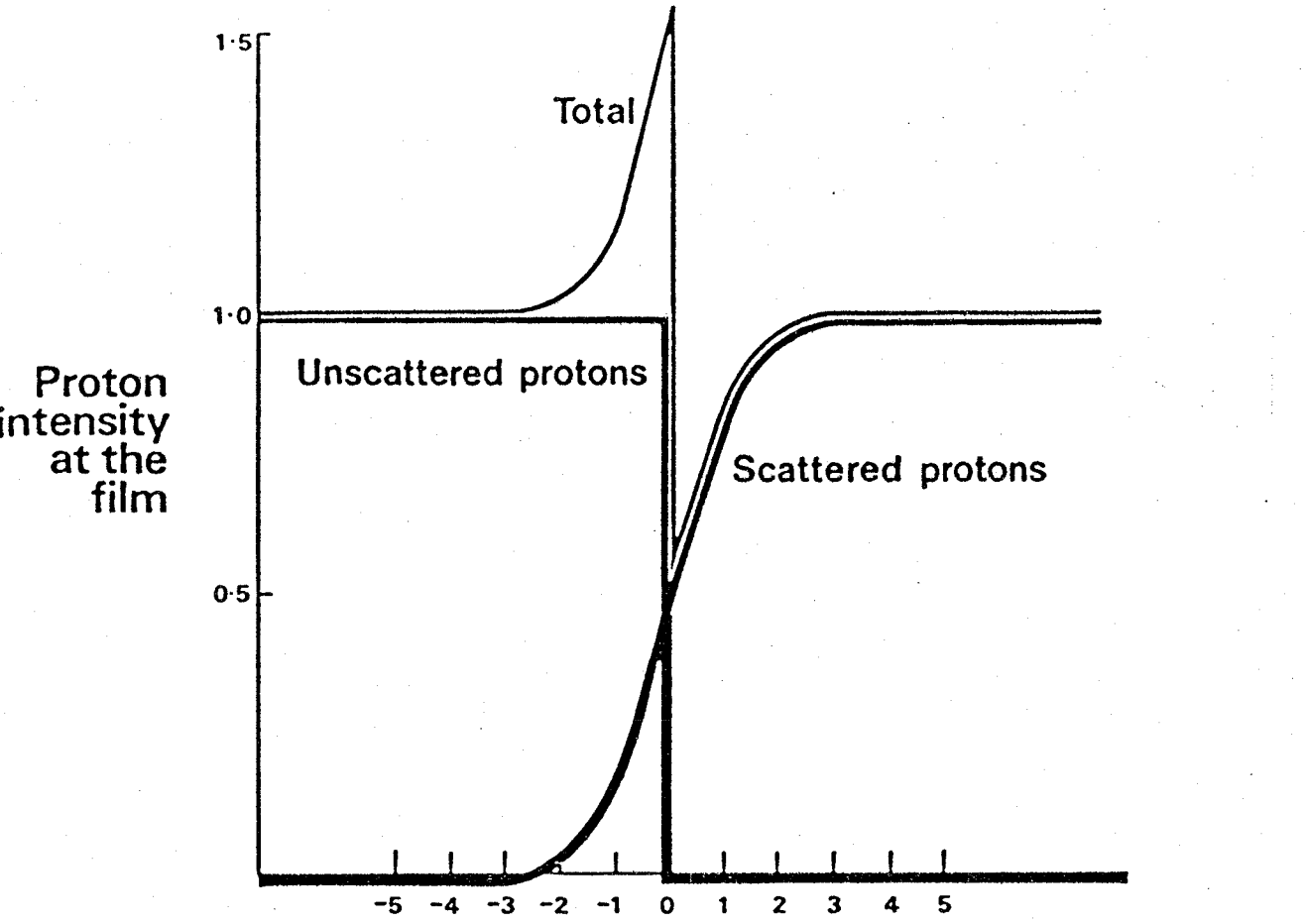

where ℓ = distance of the film behind the edge
θs = root mean square scattering angle of the protons in the thickness of the matter comprising the edge

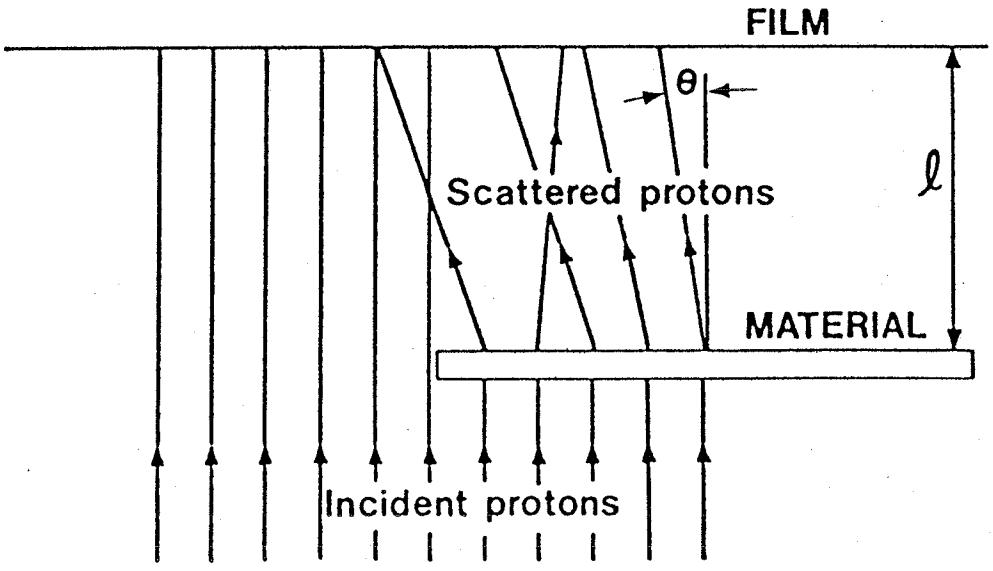

Figure 12: The Intensity Pattern Behind an Edge as a Result of Proton Scattering

II.2 THE BARLEY GRAIN

Barley grains subjected to hydrostatic pressures similar to those that they experience during the production of malt were observed to suffer a reduction in their respiratory activity and germination rate. This was apparently caused by water being forced into the embryos by the pressure, although no evidence for this was found on the surface of the grain. This matter is of considerable concern as malting processes generally take place in deep vats, exposing the grains to hydrostatic pressures of up to 200 kPa. The result of these effects is a general reduction in the yield of malt (Th84).

In the process of studying the hydrostatic pressure effects in steeped barley relating to water sensitivity, G.D. Thraves and W. Woodbury of the Department of Plant Sciences at the University of Manitoba approached the cyclotron laboratory for assistance.

There is a structure at the tip of the barley grain that is believed to be a factor in the above-mentioned process. It is not possible to physically determine the structure of this compartment within the seed as it collapses when the grain is dissected (Wo84). It was hoped that the internal structure could be determined by means of proton radiography.

II.3 EXPERIMENTAL PROCEDURE AND RESULTS

The proton radiography was conducted on beam-line D as shown in figure 4. The apparatus consisted essentially of a modified 35 mm camera which was placed in the beam line. The grains were mounted on the face of the camera and were seperated from the film itself by only a thin aluminum plate. Thus, 'contact radiographs', akin to the contact prints that one produces of photographic negatives, are produced.

The experimental arrangement is illustrated in figure 13. An experimental cube placed in the beam line is open to air. Kapton windows seal the vacuum in the beam pipe on either side of the cube. The camera is then placed in the cube to be illuminated.

Several types of films and papers were used for exposure to the proton beam and printing of the negatives, respectively. The best results and greatest detail were obtained with Kodak Tech-Pan film and medium weight, glossy Kodabrome II RC paper with extra-hard contrast (F4). Kodak Microdol-X developer, a fine-grain developer, was used to process the irradiated negative to enhance the detail. Samples of the results are shown in figure 14. The outline of the grains can be seen fairly readily and some internal detail is discernable.

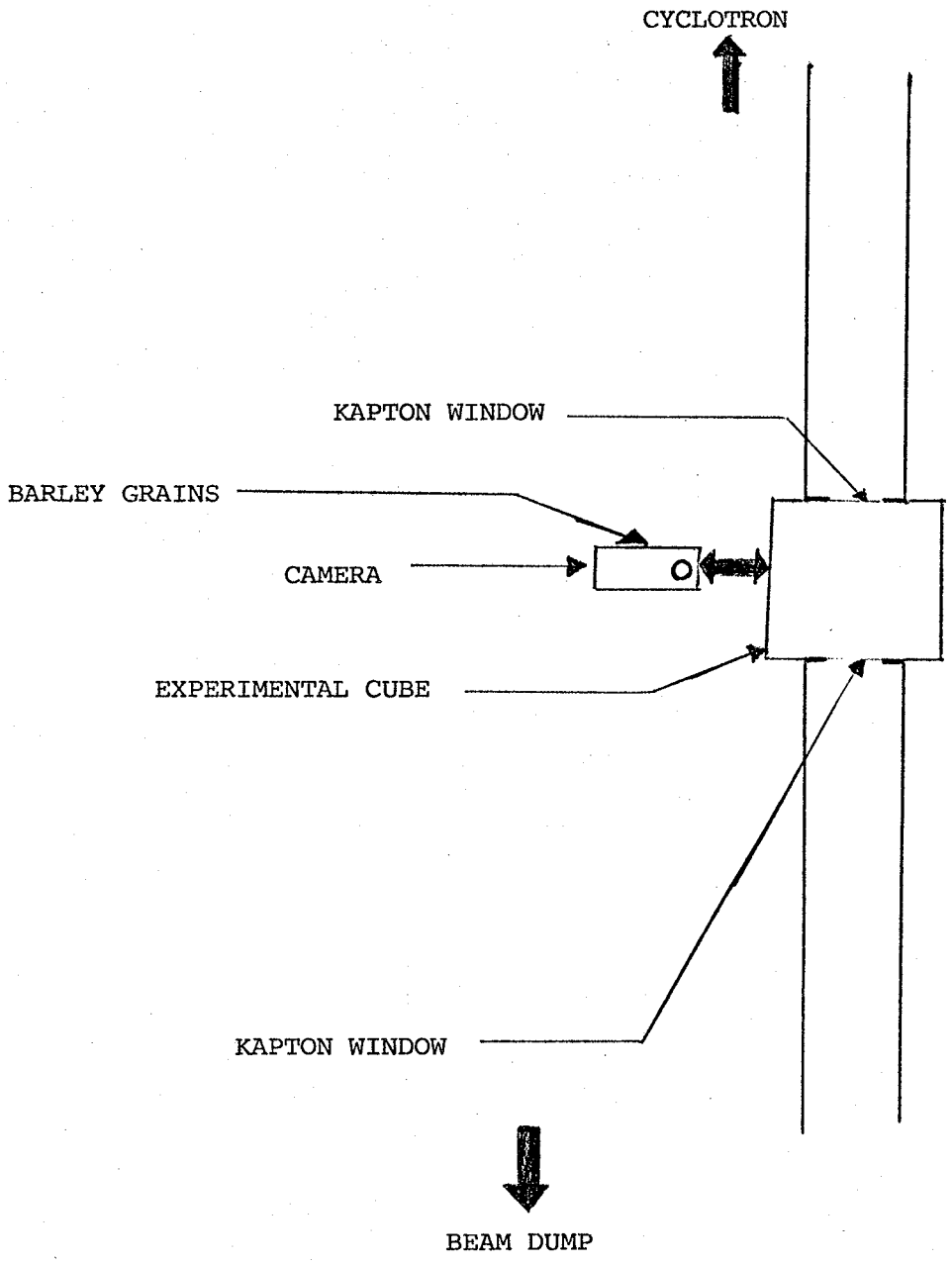

Figure 13: Experimental Arrangement for Proton Radiography Experiment on 'D' Line

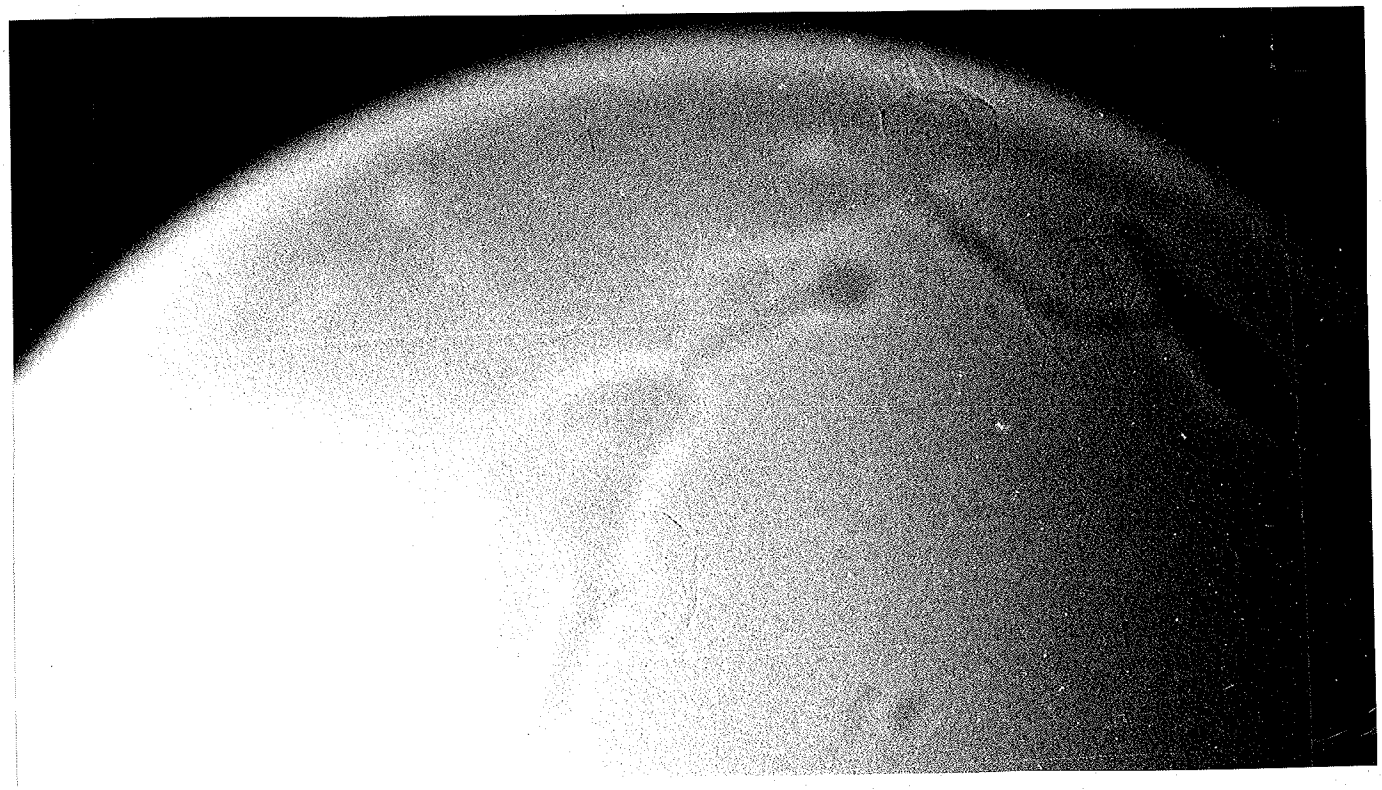

Figure 14: Proton Radiograph of Barley Tips

II.4 SUMMARY

It has been shown that proton scattering radiography can be conducted at the University of Manitoba Cyclotron Laboratory. Although further resolution is desired, the process itself has been proven. Improvements may result from the use of specialized films designed for radiographic studies and from the construction of a modified, automated target system to replace the camera currently in use.

CHAPTER III

DESIGN OF A SEPARATED TURN EXTRACTION SYSTEM FOR DEUTERONS

III.1 INTRODUCTION

During the acceleration of any given 'bunch' of deuterons in a cyclotron, the particles being accelerated experience an energy spread as they do not all follow the reference ray, the optic axis. Those particles that arrive ahead or behind the reference particle with respect to time will gain different amounts of energy from the accelerating radio frequency (rf) field.

As a particle is accelerated, the voltage gain per turn depends upon the exact phase of the particle relative to the radio frequency accelerating voltage, and as a result, the different components of a single beam bunch will gain different amounts of energy as they are accelerated. When a particle passes through an accelerating gap, the radius of curvature increases, resulting in a corresponding displacement of the

centre of curvature of that particle's trajectory. Thus, as particles with different energies move along different radii, the energy spread can be expressed in terms of the centre spread. By the time the beam is extracted, orbits overlap each other to the extent that they cannot easily be distinguished (Oh84).

In order to reduce the center spread, a two stage separated turn extraction system has been designed for deuterons. The University of Manitoba cyclotron is now able to provide deuteron beams with better than 50 keV resolution up to an energy of 15 MeV. Above 15 MeV, simulated single turn extraction is no longer possible.

III.2 STAGE 1 - COLLIMATORS

Two collimators are placed so as to intercept the first orbits of the injected beam and stop those particles far removed from the reference ray.

In order to position these slits accurately and precisely, and also to remove them when not in use, some type of motor drive is required. Since a conventional motor could be disabled in the strong magnetic field of the cyclotron, and

could in turn upset the carefully balanced magnetic field, it was suggested that a homopolar motor (Figure 15) be used. This is essentially a non-magnetic metallic disk, known as a Faraday disk, placed in a magnetic field as shown. Applying a current across the radius of the disk causes the motor to revolve. The high revolutions of this Faraday disk are reduced by means of a gear train, which in the process increases the final torque delivered to the collimator assembly. The motion of the collimator is then determined by remotely adjusting the current that is applied across the disk. The collimators are most effective when they are placed 90° apart in the plane of the particles' motion (Oh84).

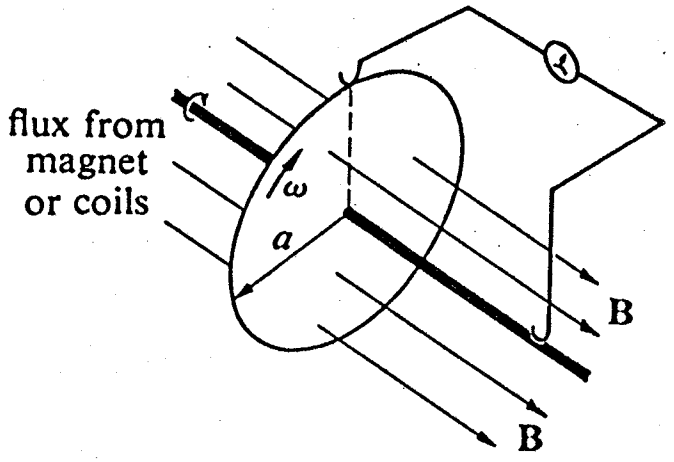

Figure 15: Faraday's Disk

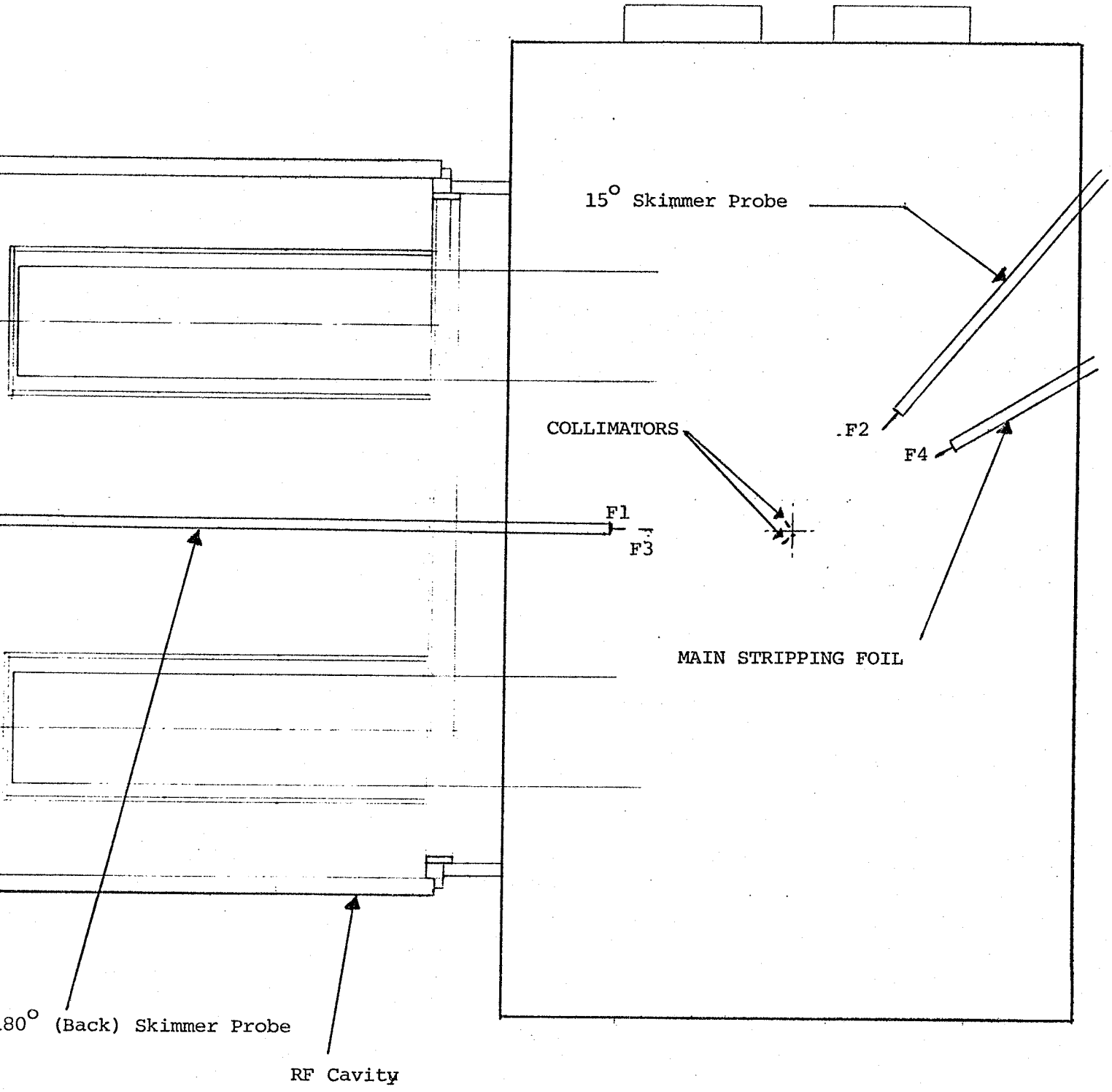

Figure 16: Schematic of Seperated Turn Extraction System for Deuterons

III.3 STAGE II - SKIMMER PROBES

Although the beam is collimated immediately after injection, it can still have a considerable centre spread at extraction. Thus, it is neccessary to trim the beam so that only a highly resolved beam (with respect to energy) encounters the stripping foil. To accomplish this, one adds two specially designed stripping foils, or skimmer probes, to intercept the beam during its last orbit (the 130th turn for 15 MeV D^- ions), as shown in figure 16.

15 MeV deuterons are extracted at a radius of 35 cm, at which point the particles have gained approximately 138.6 keV per turn. Thus the distance between the last two orbits, ΔR, is given by (Oh84)

$$\Delta R = \frac{R \Delta E}{2E} \qquad \text{(III-1)}$$

and is found to be approximately 1.6 mm.

D ions which pass F2 within 0.5 mm and pass through the gap in F1 can reach the main stripping foil, F3, and be extracted. Therefore the center of curvature of the ions has to be within the limits set by

$$\Delta_c r_{max} = \frac{0.25 \text{ mm}}{2} + \frac{0.25 \text{ mm}}{2} = 0.25 \text{ mm}$$

$$\Delta_c r_{max} = \frac{-0.25 \text{ mm}}{2} - \frac{0.25 \text{ mm}}{2} = -0.25 \text{ mm}$$

therefore

$$\Delta r = \frac{0.25}{2} - \frac{0.25}{2} = 0.00$$

For Δ_c r=0 ions,

$\Delta r_{max} = 0.25$ mm $\qquad E_{max} = 21.4$ keV

$\Delta r_{min} = -0.25$ mm $\qquad E_{min} = -21.4$ keV

This gives a final energy spread on the order of 50 keV.

III.4 SKIMMER PROBE DESIGN

F3 is the main stripping foil currently used for normal extraction of the beam. F1 is actually a stripping foil with a 0.5 mm slit in the centre to permit passage of the beam of the correct energy.

The skimmer foil F2 is attached to a probe arm mounted at 15 to the main stripping foil probe and uses largely the same design as the main stripping foil for remote angle and radius positioning and readout. However, the tip has been redesigned (Figure 17) to allow the foil to enter the cyclotron below the median plane, and thus under the beam extracted by F4. The foil may then be raised remotely by means of the wire indicated, which also allows one to read the current of the beam intercepted by this foil.

The back probe, upon which is mounted foil F1, does not require angular adjustment, although its radius is to be adjusted with respect to the energy of the extracted particles. A sectional probe which enters from behind the RF box, and which will be supported within this cavity, is to be adapted for this purpose.

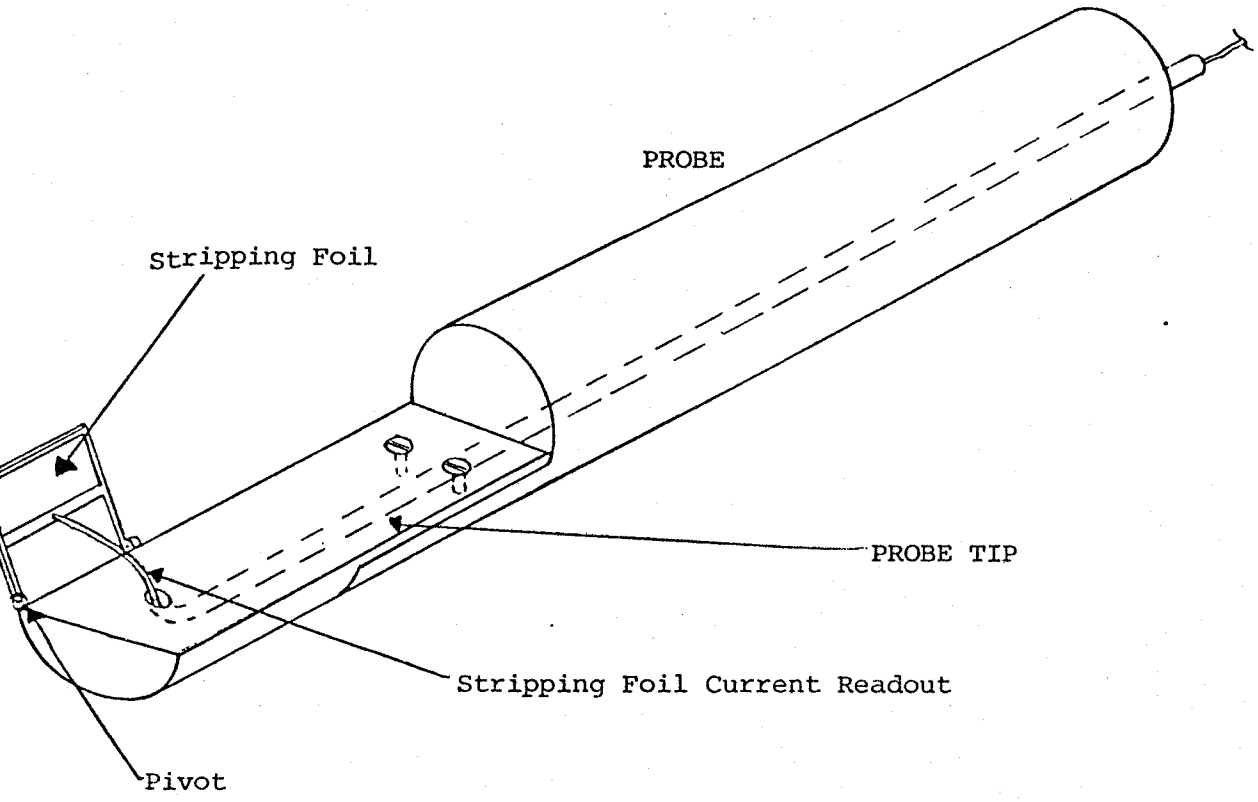

Figure 17: 15^{o} Probe Tip (Skimmer Probe)

Considerable additional shielding will be required around the areas of the machine receiving beam that is removed by the skimmer probes.

An advantage of this apparatus is that F2 may be used in the future for dual extraction of either deuterons or protons. There are plans to transmit this beam down a second beamline, 15 removed from the main beamline, directly into the vault. This line can then be used for the production of radioisotopes simultaneously with the conduct of a nuclear physics experiment in one of the experimental areas.

The detailed designs for skimmer probes are currently being drafted and the entire system for the seperated turn extraction of deuterons should be on line and operational late in 1985.

SUMMARY AND CONCLUSION

A high energy proton microbeam system has been designed, consisting of a series of collimators and magnetic quadrupole lenses. The collimators have been built, the final design for the slit faces being that first used by Nobiling. The four quadrupole magnets will be used in the 'Russian Quadruplet' configuration of Dymnikov. They are currently under construction and are to be completed late in 1985.

Proton radiography has been investigated for use as an analytical tool in research. Radiographs have been made of barley grains in order to discern features of their internal structure. Certain internal structure is visible, but further clarification of detail is neccessary to prove the viability of this process. Such developments are currently in progress.

The University of Manitoba cyclotron has recently been modified to produce deuteron beams of up to 26 MeV. In order to improve the quality of this beam, a simulated single-turn extraction system has been proposed and is currently in various stages of design and construction. This system consists of two collimators that intercept the first orbit of the beam and two additional stripping foils that skim the beam in its last orbit before extraction. The resulting deuteron beams will have an

energy resolution of better than 50 keV up to an energy of 15 MeV.

BIBLIOGRAPHY

(Ba82) S.L. Balasko, Masters Thesis, Faculty of Human Ecology, University of Manitoba, 1982

(Ca80) T.A. Cahill, Ann. Rev. Nucl. Part. Sci. 30 (1980) 211

(Co72) J.A. Cookson, A.T.G. Ferguson and F.D. Piling, J. Radioanal. Chem. 12 (1972) 39

(Co79) J.A. Cookson, Nucl. Instr. and Meth. 165 (1979) 477

(Dy65) A.D. Dymnikov, T. Ya. Fishkova and S. Ya. Yavor, Sov. Phys. Tech. Phys. 10 (1965) 340

(Ha84) F. Hawthorne, Department of Earth Sciences, University of Manitoba, Personal Communication, 1984

(Ko68) A.M. Koehler, Science, 160 (1968) 303

(La81) C. Lapointe, Masters Thesis, Department of Physics, University of Manitoba, 1981

(Le82) G.J.F. Legge, Nucl. Instr. and Meth. 197 (1982) 243

(Le84) G.J.F. Legge, Nucl. Instr. and Meth. 231[B3] (1984) 561

(Mc81) J.S.C. McKee, C. Lapointe, J. Birchall, C. Pinsky and R. Bose, J. Envir. Sci. and Health (Part A) 16[5] (1981) 465

(Mc83) J.S.C. McKee, R. Bose, G.D. Sharma, D. Gallop, J.J.G. Durocher, I.M. Gusdal and C. Pinsky, Can. Nucl. Ass. 4th Ann. Conf. Proc., June 15 1983, 2, J1

(No75) R. Nobiling, Y. Civelekoglu, B. Pohl, D. Schwalm and K. Traxel, Nucl. Instr. and Meth. 130 (1975) 325

(Oh84) S. Oh, Department of Physics, University of Manitoba, Personal Communication, 1984

(Pr85) R. Prakash, J.S.C McKee, Nucl. Instr. and Meth. (1985), in press

(St79) V.W. Steward, IEEE Transactions on Nuclear Science, NS-26(No. 2) (1979) 2257

(Ti78) P.A. Tipler, Modern Physics, Worth Publishers Inc., 1978

(Th84) G.D. Thraves, Masters Thesis, Department of Plant Science, University of Manitoba, 1984

(We72) D. West, A.C. Sherwood, Nature 239 (1972) 157

(We75) D. West, Atom 222 (1975) 54

(Wi77) S.F.J. Wilk, J.S.C. McKee and C.P. Randell, Nucl. Instr. and Meth. 142 (1977) 33

(Wo73) R. Woldseth, All You Ever Wanted to Know About XES, Kevex Corporation, 1973

(Wo84) W. Woodbury, Department of Plant Science, University of Manitoba, Personal Communication, 1984

(Zi53) R.E. Zirkle and W. Bloom, Science 117 (1953) 487